LIMNOLOGY and OCEANOGRAPHY

ASLO

Limnol. Oceanogr. 66, 2021, 878–891

doi: 10.1002/lno.11648

Nitrate promotes the transfer of methane-derived carbon from the methanotroph *Methylobacter* sp. to the methylotroph *Methylotenera* sp. in eutrophic lake water

Sigrid van Grinsven,[1*] **Jaap S. Sinninghe Damsté**,[1,2] **John Harrison**,[3] **Lubos Polerecky**,[2] **Laura Villanueva**[1,2]

[1]Department of Marine Microbiology and Biogeochemistry, NIOZ Royal Netherlands Institute for Sea Research, Den Burg, The Netherlands
[2]Department of Earth Sciences, Faculty of Geosciences, Utrecht University, Utrecht, The Netherlands
[3]Washington State University Vancouver, School of the Environment, Vancouver, Washington

Abstract

Eutrophic lakes are major contributors to global aquatic methane emissions. Methanotrophy, performed by methane oxidizing bacteria, results in the production of biomass, fermentation products and/or CO_2, making methane-derived carbon available to non-methanotrophic organisms. Methanotrophs can co-occur with methylotrophs which are expected to consume methane-derived carbon. However, it is unknown if this interaction requires cell-to-cell contact, whether physicochemical factors affect this interaction, and what role this interaction may play in ecosystems and biogeochemical cycling in lakes. Here, we performed incubations of an enrichment culture obtained from a eutrophic lake with ^{13}C-labeled methane, revealing the transfer of methane-derived carbon from the methanotroph *Methylobacter* sp. to a methylotroph of the genus *Methylotenera*. These microorganisms occurred both in mixed clusters and as single cells, indicating that their interaction does not require physical cell contact. In addition, the carbon transfer between the partners is dependent on the presence of nitrate, which is potentially used by *Methylotenera* sp. and in turn may affect the methane oxidation rate of *Methylobacter* sp. This interaction, and its dependence on nitrate, may have important implications for the carbon cycle in eutrophic lakes worldwide.

Methane, the most important anthropogenic greenhouse gas after CO_2 (Stocker et al. 2013), is emitted to the atmosphere by numerous sources, both anthropogenic and natural, among which aquatic systems such as wetlands, lakes, and reservoirs contribute about 16–23% to global methane emissions (Bastviken et al. 2011; Saunois et al. 2016; DelSontro et al. 2018). Methane production in aquatic systems occurs naturally, but its emission rates can be strongly influenced by human impacts such as eutrophication and warming (Yvon-Durocher et al. 2014; Deemer et al. 2016). Methane consumption by microbes (i.e., methanotrophy) is performed by either archaea or bacteria occupying distinct ecological niches, consuming a substantial portion of the produced methane (Bastviken et al. 2008). Methane oxidizing bacteria are mostly aerobes, with certain species capable of methane oxidation under anoxic conditions, by using nitrite (Ettwig et al. 2010), nitrate (Kits et al. 2015), sulfate (Schubert et al. 2011), and possibly humic substances as electron acceptors (Saxton et al. 2016).

Methane oxidation is a key process in the carbon cycle of shallow, eutrophic lakes. The majority of aquatic organisms, both bacteria and species of higher trophic levels, are unable to use methane directly. They are therefore dependent on the conversion of methane into other carbon compounds by methane oxidizing bacteria, which can be a major component of the carbon budget of lake water columns, comparable to the contribution of phytoplankton primary production (Taipale et al. 2011). Methane oxidation by methane oxidizing bacteria proceeds, besides biomass, mostly to carbon dioxide (Murrell 2010), although recent studies have shown that methane oxidizing bacteria can perform mixed-acid fermentation in anoxic environments resulting in excretion of other reaction products such as acetate, succinate and H_2 (Kalyuzhnaya et al. 2013; van Grinsven et al. 2020*a*). Some studies have shown that methane oxidizing bacteria can

*Correspondence: sigrid.van.grinsven@nioz.nl

Additional Supporting Information may be found in the online version of this article.

perform mixed-acid fermentation in anoxic environments resulting in excretion of other reaction products such as acetate, succinate and H_2 (Kalyuzhnaya et al. 2013; van Grinsven et al. 2020*a*). However, it is still held that most methane utilized by methane oxidizing bacteria is either converted to CO_2 or incorporated into biomass (Murrell 2010). It has also been shown that intermediates of the methane oxidation reaction, such as methanol and formaldehyde, can be excreted into the ecosystem (Xin et al. 2007; Tavormina et al. 2017) and further used as a carbon source by non-methanotrophic microorganisms. This conversion and subsequent excretion may have implications for the microbial food web as higher trophic levels have been shown to consume high amounts of methane-derived carbon (Jones et al. 1999; Murase and Frenzel 2007; Jones and Grey 2011; Sanseverino et al. 2012; He et al. 2015). The release of methanol, however, leads to an energy deficiency in the methanotrophic cell, as the conversion of methane to methanol is energy consuming. Energy is only gained at further steps in the methane metabolism (Xin et al. 2004, 2007). It is, therefore, unclear whether there is a gain for the methanotrophs in the excretion of methanol.

Methylotrophs (i.e., microbes consuming single-carbon compounds) of the genera *Methylophilus* and *Methylotenera* have been shown to co-occur with methanotrophs, and it has further been suggested that methylotrophs consume methanotroph-derived methanol (Oshkin et al. 2014). A study by Krause et al. (2017) with synthetic co-cultures, established with isolates from lake sediment, suggested a cross-feeding mechanism in which the methylotroph induces a change in gene expression of the methanotroph, resulting in release of methanol to support methylotroph growth. However, it is unknown (1) whether there is a gain for the methanotroph, either through a transfer of vitamins or direct interspecies electron transfer as previously suggested (Yu and Chistoserdova 2017), and (2) if this interaction requires a physical contact between the partners. Also, the effect of the physicochemical environmental conditions on this presumed partnership has not yet been determined.

In this study, we further investigated the transfer of methane-derived carbon in an enrichment culture, obtained from the water column of a eutrophic lake, which was dominated by the methanotroph *Methylobacter* sp. and a non-methanotrophic methylotroph of the genus *Methylotenera*. Physical contact between the partners is not essential for the transfer of carbon between the two organisms, as was confirmed by Stable isotope probing (SIP) and Nanoscale Secondary Ion Mass Spectrometry (NanoSIMS). Up to now, studies have focused on artificial, non-complex communities, or soil/sediment systems (Martineau et al. 2010; Hernandez et al. 2015; Wei et al. 2016*a*). Here, we present the first visualization of the co-occurrence, and possible partnership, of *Methylobacter* and *Methylotenera* sp. in a water column enrichment. Furthermore, our results suggest a link between nitrogen and carbon cycles wherein nitrate stimulates methane oxidation and the transfer of associated carbon compounds. It is possible these processes could in-turn affect the trophic transfer of methane-derived carbon in lake systems. Hence, our results have implications for methane cycling, for the wider community and trophic dynamics, and the carbon balance of temperate eutrophic lakes.

Material and methods

Sample collection, enrichment and incubation experiments

Enrichment cultures were established as described in van Grinsven et al. (2020*b*). Briefly, suspended particulate matter from the oxic water column of Lacamas Lake (Washington) was collected by filtration through a 0.7 μm pore size glass fiber GF/F filter, transferred to nitrate mineral salts medium (Whittenbury et al. 1970), and supplied with methane (99.99% purity). After 12 weeks at 15°C, during which the culture was transferred six times, the larger cell clusters were separated from the smaller clusters and single cells by filtration over a 10 μm filter in an attempt to separate and enrich specific species based on cluster size. Subsequently, both fractions were resuspended in nitrate mineral salts media and treated similarly to the earlier subcultures. After 8 weeks, the cells of each culture (named "Particle culture" and "Filtrate culture") were harvested by gentle centrifugation (2800 × *g* for 5 min, 15°C) and used as inoculum for incubation experiments. A sample of each inoculum was stored for DNA-analysis.

Incubation experiments were supplied with 100% ^{13}C-labeled methane (Sigma-Aldrich), in the absence and presence of nitrate as described for the "particle culture" in van Grinsven et al. (2020*b*). The procedure for the "filtrate culture" was identical. Briefly, incubation experiments with nitrate were performed with oxic nitrate mineral salts medium, which was also used for cultivation as described above, containing nitrate as the only nitrogen source (Whittenbury et al. 1970). Ammonium incubations were performed with an oxic ammonium mineral salts medium, containing ammonium rather than nitrate as nitrogen source (1 g L^{-1} KNO_3 was replaced with 0.5 g L^{-1} NH_4Cl, as described by Whittenbury et al. 1970). All incubation experiments were performed in triplicate in 260 mL acid-washed and autoclaved glass pressure bottles with butyl stoppers, containing 200 mL media and 2.6 mL 100% ^{13}C-labeled methane (10% v/v methane, Sigma-Aldrich) in the air headspace, at atmospheric pressure. All incubations were performed at 15°C in the dark, lasting 2–3 d. Daily measurements of the headspace methane concentration of oxic incubations ("particle" and "filtrate" culture) were performed via gas chromatography with a flame ionization detector (GC-FID), as described in van Grinsven et al. (2020*b*). Calculations showed that the oxygen concentration (± 640 mM) was, assuming methanotrophy was the only process consuming oxygen, present in surplus (van Grinsven et al. 2020*b*). At termination, samples were taken for visual analysis of both

cultures, as described below, and, for the incubations with the "particle culture," for determination of the NH_4^+, NO_3^-, and NO_2^- concentrations by Continuous Flow Analyses, performed on a QuAAtro Segmented Flow Analyzer (Seal Analytical). All incubation experiments were then terminated by filtering onto polycarbonate filters (47 mm diameter, 0.2 μm pore size; Millipore). Filters were stored at − 80°C until DNA extraction using the RNeasy Powersoil Total RNA extraction + DNA elution kit. DNA extracts were stored at − 20°C until further processing.

Sample preparation for DNA stable isotope probing analysis

Samples from the "particle culture" incubation experiments were used for DNA-SIP analysis. Fraction separation was performed by CsCl density gradient centrifugation of the total DNA, as described in detail by Suominen et al. (2020), following the protocol of Dunford and Neufeld (2010). Briefly, 4 μg of total DNA was added to a CsCl solution, obtaining a final density of 1.725 g ml^{-1}, which was put in 5.1 mL QuickSeal Polyallomer tubes (Beckman Coulter, Brea, California). The samples were centrifuged for 60 h at 44,000 rpm (177,000 × *g*) at 20°C using a Vti 65.2 rotor (Beckmann Coulter, Brea, California). The CsCl solution, containing the DNA, was then divided into 12 equal fractions, and the gradient formation was checked by measuring the density of a 10 μL sub-sample of each fraction with a digital refractometer (AR2000 Reichert Technologies, Buffalo, New York). To precipitate the collected DNA, two volumes of a polyethylene glycol solution were added (30% PEG6000, 1.6 M NaCl) together with 20 μg of polyacrylamide as a carrier, followed by incubating at room temperature for 2 h and pelleting the DNA by centrifugation at 13,000 × *g* for 30 min at 4°C. Pellets were washed with 70% ethanol, air-dried and resuspended in PCR-grade water.

16S rRNA gene amplification, data processing and quantification

Both DNA extracted directly from the incubation experiments and DNA that was obtained after the DNA-SIP procedure were used for PCR amplification by using the general 16S rRNA archaeal and bacteria primer pair 515F and 806RB targeting the V4 region (Table S1; Caporaso et al. 2012) as described in van Grinsven et al. (2020*b*). Briefly, after amplification, the PCR products were gel-purified using the QIAquick Gel-Purification kit (Qiagen) and pooled and diluted. Sequencing was performed by the Utrecht Sequencing Facility (Utrecht, the Netherlands), using an Illumina MiSeq sequencing platform. The Cascabel pipeline was used for the analysis of the 16S rRNA gene amplicon sequences (Asbun et al. 2019). This included quality assessment by FastQC (Andrews et al. 2015), assembly of the paired-end reads with Pear (Zhang et al. 2014), and assignment of taxonomy (including pick representative set of sequences with "longest" method) with blast using the Silva 132 release as reference database (Quast et al. 2013, https://www.arb-silva.de/). The 16S rRNA amplicon reads (raw data) have been deposited in the NCBI Sequence Read Archive (SRA) under BioProject number PRJNA603000.

16S rRNA gene copies were quantified using quantitative PCR (qPCR) with the same primer pair as used for amplicon sequencing (515F, 806RB). The qPCR reaction mixture (25 μL) contained 1 U of Pico Maxx high fidelity DNA polymerase (Stratagene, Agilent Technologies, Santa Clara, California), 2.5 μL of 10× Pico Maxx PCR buffer, 2.5 μL of each dNTP (2.5 mM), 0.5 μL BSA (20 mg mL^{-1}), 0.02 pmol μL^{-1} of primers, SYBR Green® (Invitrogen) diluted 10,000-fold (optimized concentration), 0.5 μL of 50 mM $MgCl_2$ stock solution, and ultrapure sterile water. The cycling conditions for the qPCR reaction were as follow: initial denaturation 98°C for 30 s, 45 cycles of 98°C for 10 s, 56°C for 20 s, followed by a plate read, 72°C for 30 s, and 80°C for 25 s. Specificity of the reaction was tested with a gradient melting temperature assay, from 55°C to 95°C with 0.5°C increments of 5 s apiece. The qPCR reactions were performed in triplicate with standard curves encompassing a range from 10^0 to 10^7 molecules μL^{-1}. qPCR efficiency for the 16S rRNA gene quantification was 103.7% with $R^2 = 0.996$.

The 16S rRNA gene sequencing and the qPCR data of the DNA-SIP experiment were combined with the measured density of each DNA-SIP fraction to calculate the average density of specific species (*Methylobacter*, *Methylotenera* and *Flavobacterium*) per treatment (ammonium or nitrate amended incubations, only for the "particle culture").

CARD-FISH and imaging

Cells for catalyzed reporter deposition fluorescence in situ hybridization (CARD-FISH) analysis were collected at the end of incubation experiment (i.e., for both the "particle" and "filtrate" cultures) by transferring 10 mL of medium to a 50 mL tube. Formaldehyde was added to a final concentration of 4% and the tubes were left overnight at 4°C to fixate the cells. The formaldehyde-fixed cells of the ammonium- and nitrate-supplemented incubation experiments were deposited onto gold-coated polycarbonate filters, other samples were deposited on non-coated polycarbonate filters (both 0.45 μm pore size). Cell density was checked with SybrGreen staining after which filters were used for CARD-FISH. In short, cells were embedded in low-melting point agarose before being permeabilized using lysozyme (10 g L^{-1}) for 1 h at 37°C. Probes (50 ng μL^{-1}) were mixed with hybridization buffer in a 1 : 200 ratio. Filters were incubated with hybridization mix for 18 h at 35°C. Probe details are shown in Table S1. Because the Illumina 16S rRNA gene sequence analyzed does not coincide with the sequence location of the probes, we compared 16S rRNA gene sequences closely related to the *Methylobacter* and *Methylotenera* representative OTUs present in the enrichment (van Grinsven et al. 2020*b*). This comparison resulted in 100% match (Table S1), validating that the probe sequences for

Methylobacter and *Methylotenera* fitted the specific species in our samples. Dyes Alexa 488 and Alexa 555 were used in the amplification step. The complete protocol can be found at https://www.arb-silva.de/fish-probes/fish-protocols.

After CARD-FISH staining, filters were viewed and imaged using an Axioplan microscope with fluorescence filters L09 (BP 450/490 nm, FT 510 nm, LP 520 nm) and Cy3 (BP 535/50 nm, FT 620/25 nm, LP 565 nm). Images of cells that were used in this publication were taken with either the Axioplan microscope or using a Nikon Eclipse Ti microscope with an ET-mCherry filter at the Utrecht University Biology Imaging Centre.

NanoSIMS data collection and processing

Analysis by Nanoscale Secondary Ion Mass Spectrometry (NanoSIMS) was performed with the NanoSIMS 50 liter instrument (Cameca, Gennevilliers, France) operated at Utrecht University, using the same filters as treated and imaged for CARD-FISH. First, areas on the filter containing target cells were located by fluorescence microscopy (see above) and marked using photo-ablation. This helped their localization in the NanoSIMS instrument. Each area of interest (squares of 20–40 μm in size) was first pre-sputtered until secondary ion yields stabilized. Afterwards, the area was rasterred multiple times (typically 20–80 planes) with a Cs^+ primary ion beam (1–2 pA, dwell time of 1 ms pixel^{-1}) while detecting the secondary ions $^{12}C^{14}N^-$ and $^{13}C^{14}N^-$ with separate electron multiplier detectors. NanoSIMS data was processed with the Look@NanoSIMS software (Polerecky et al. 2012). After alignment of individual planes, regions of interest corresponding to individual cells were drawn manually based on the $^{12}C^{14}N$ ion counts, which represent biomass. Subsequently, the cellular ^{13}C atom fraction was evaluated from the total ion counts of $^{13}C^{14}N$ and $^{12}C^{14}N$ accumulated over the regions of interest pixels as $x(^{13}C) = {}^{13}C^{14}N/({}^{13}C^{14}N + {}^{12}C^{14}N)$. Region of interest classification as *Methylobacter*, *Methylotenera* and "others" was done based on the overlay of the NanoSIMS and fluorescence (CARD-FISH) images. A sample of the culture not grown on $^{13}CH_4$ was used as a control (Fig. S1). Due to the low number of imaged cells and the non-random selection of scanned areas, we did not attempt to perform statistical analysis on NanoSIMS data.

Results

The experimental procedures that resulted in the establishment of the two enrichment cultures used for this study have been described previously (van Grinsven et al. 2020*a*,*b*). Briefly, the first enrichment culture ("particle culture") was dominated by 16S rRNA gene sequences affiliated with the methanotroph *Methylobacter* sp. (43%) and with the methanol-oxidizing methylotroph *Methylotenera* sp. (21%; Fig. S2), and was obtained from the mixed winter water column of the eutrophic Lacamas Lake (van Grinsven et al. 2020*b*). This culture was used to perform incubation studies under oxic/anoxic conditions with the addition of ammonium or nitrate as nitrogen source as previously reported, showing methane oxidation occurred under oxic, but not under anoxic conditions (van Grinsven et al. 2020*b*; Fig. S2; Table S2). The aerobic methane oxidation rate was enhanced by the presence of nitrate (van Grinsven et al. 2020*b*). The *Methylobacter* sp. 16S rRNA gene sequences from the enrichment culture, as well as from natural waters, field and laboratory incubation experiments (van Grinsven et al. 2020*a*,*b*), formed a subcluster of closely related sequences (i.e., 96–99% similarity) within the *Methylobacter* sp. clade 2 cluster (described in Smith et al. 2018). Besides this *Methylobacter* sp.-dominated enrichment culture, a second enrichment culture ("filtrate culture"; Fig. S2; Table S2) was obtained with similar relative abundances of *Methylotenera* sp. and total methanotrophs, but rather than being dominated by *Methylobacter* sp., the methanotrophic community consisted of both *Methylobacter* and *Methylomonas* spp.

^{13}C-label incorporation analysis by DNA-SIP

The "particle enrichment culture" (containing 43% *Methylobacter* sp. and 21% *Methylotenera* sp., Fig. S2) was used for incubation experiments with ^{13}C-labeled methane to be able to follow the incorporation of methane-derived carbon into the DNA of the microbial community by using DNA-SIP. In both the incubation experiments with ammonium and nitrate, ^{13}C-methane was the only external carbon source, as no CO_2 was added and the experiments were performed in the dark to exclude phototrophic CO_2 fixation and oxygen production. ^{13}C-enrichment of the cells will increase the molecular weight of the DNA, causing the DNA to end up in higher density fractions compared to unlabeled DNA of the same species. An increase in the average density, and thus in ^{13}C-enrichment, was observed for both the *Methylobacter* and *Methylotenera* genera in the incubations with nitrate, compared to the incubations with ammonium (Fig. 1). *Flavobacterium* spp., which comprised 6–8% of the total 16S rRNA gene reads in the various incubations, remained unlabeled and showed a similar average density in both incubations (Fig. 1). The difference in average density between *Methylobacter* and *Methylotenera* spp. in the ammonium incubations could partly be explained by the natural average density difference between the species (Fig. S3), but likely also results from label uptake by *Methylobacter* sp. but not *Methylotenera* sp. in the ammonium incubations, given the high methane turnover rate and the enlarged difference in average density between the species (cf. Figs. 1, S3).

Visualization of *Methylobacter* and *Methylotenera* cells

Microbial cells were identified using CARD-FISH with probes Mlb482 (targeting *Methylobacter*) and MET1216 (targeting the family *Methylophilaceae*, which, in our incubation experiments, was dominated by the genus *Methylotenera*, with < 3%

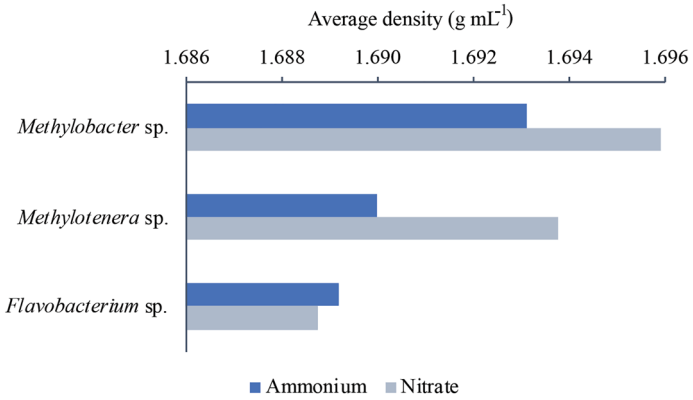

Fig 1. Average density (in g mL^{-1}) of *Methylobacter* sp., *Methylotenera* sp., and *Flavobacterium* sp. DNA fractions as observed in the DNA stable isotope probing analysis of the incubation experiments with the "particle enrichment culture" amended with ammonium and nitrate. The natural difference in density among the species is shown in Fig. S3.

of *Methylophilaceae* 16S rRNA reads belonging to non-*Methylotenera* genera). Both *Methylobacter* and *Methylophilaceae* (from here on called *Methylotenera*) cells were abundant in the incubations with ammonium and nitrate, of both the "particle" and "filtrate" cultures, with *Methylobacter* cells more abundant than *Methylotenera* cells, based on visual assessment. Based on the positive CARD-FISH imaging with the Mlb482 probe, *Methylobacter* cells were rod-shaped, 2–3 μm in length and found in large and small clusters, in pairs, or as single cells (Fig. 2). Some clusters were sheet-like, with a single layer of cells (Fig. 2D), whereas other clusters were stacked in several layers and visible as piles of cells in the microscope images (Fig. 2C). *Methylotenera* cells stained with MET1216 were more variable in shape and size than the *Methylobacter* cells, and appeared in rod and cocci shapes, 1–3 μm in length. Combined clusters of *Methylobacter* and *Methylotenera* seemed to be dominated by *Methylobacter* cells, with a lower abundance of *Methylotenera* cells spread throughout the cluster (Fig. 2B, C). *Methylotenera* cells were also found as single cells (Fig. 2A), or in clusters containing only *Methylotenera* cells (Fig. 3G).

^{13}C-label incorporation analysis by NanoSIMS

Microbial assimilation of the ^{13}C-labeled carbon in the incubations with ammonium and nitrate, of both the "particle" and "filtrate" cultures, was also evaluated using NanoSIMS. This revealed ^{13}C incorporation in cells of both *Methylobacter* and *Methylotenera* spp. (Fig. 3), while all other microbial community members (i.e., not belonging to the *Methylobacter* and *Methylotenera* genera since they were not fluorescently labeled by CARD-FISH) did not show ^{13}C labeling (Figs. S1, S4). A natural abundance of ^{13}C (atom fraction 0.0105) was observed in *Methylobacter* and *Methylotenera* spp. cells grown with non-labeled methane. No difference was observed in label incorporation between the two enrichment cultures ("particle culture" and "filtrate culture"; Fig. S4). The degree of ^{13}C incorporation in *Methylobacter* and *Methylotenera* ranged widely among individual cells (^{13}C atom fractions ranging between 0.01 and 0.5). In addition, for both genera unlabeled cells were detected in the labeled-methane incubations, often in close proximity to highly ^{13}C-labeled cells (Fig. 3). ^{13}C-labeling was detected in both ammonium and nitrate-supplemented incubations and also in *Methylotenera* cells that were not in close proximity to *Methylobacter* cells (Fig. 3G–I).

Discussion

Methane-derived carbon is an important carbon source for many ecosystems (Murase and Frenzel 2007; Jones and Grey 2011; Sanseverino et al. 2012), and methanotrophs such as *Methylobacter* spp. can play a key role in the food web of aquatic systems, facilitating the transfer of methane-derived carbon up to higher trophic levels. Earlier experiments in Lacamas Lake showed high methane turnover rates (70 μmol L^{-1} d^{-1} in water column incubations, 420 μmol L^{-1} d^{-1} in enrichment culture experiments; van Grinsven et al. 2020*a*,*b*). The microbial community of the enrichment cultures obtained was dominated by *Methylobacter* and *Methylotenera* sp. (van Grinsven et al. 2020*a*,*b*; Fig. S2). Methanotrophs of the genus *Methylobacter* are commonly found in lakes, wetlands, marine systems, soils and rice paddies (Bowman et al. 1994; Smith et al. 1997; Wartiainen et al. 2006; Khmelenina et al. 2010; Wei et al. 2016*b*). Members of the *Methylotenera* genus are known for their capability to oxidize methanol, using oxygen or nitrate as an electron acceptor (Kalyuzhnaya et al. 2006; Mustakhimov et al. 2013). The suggested co-occurrence of methanotrophs and non-methanotrophic methylotrophs in Lacamas Lake is not unprecedented; it has been detected in lake systems before and has been suggested to involve a partnership based on the exchange of carbon compounds (Oshkin et al. 2014; Hernandez et al. 2015; Wei et al. 2016*a*), likely methanol (Krause et al. 2017). However, the mechanism behind the relationship between the organisms remains under debate. Most earlier studies were performed on artificial communities or co-cultures, although several studies on Lake Washington sediment microcosms suggested that a methylotroph–methanotroph partnership could be important in determining the microbial community response to changes in methane concentration in lake sediments (Beck et al. 2011; Oshkin et al. 2014; Hernandez et al. 2015). The co-occurrence of *Methylobacter* spp. and methylotrophs and the ^{13}C-labeled methane uptake by both species was also shown in Arctic sediments and soils, but the cause of the ^{13}C-labeling of the methylotroph was not further investigated (Martineau et al. 2010; He et al. 2012).

To the best of our knowledge, this study is the first one that provides direct evidence and visualization of methane-derived carbon incorporation in both species and, thus, a potential partnership of bacteria belonging to the families *Methylococcaceae* and *Methylophilaceae* in the water column of

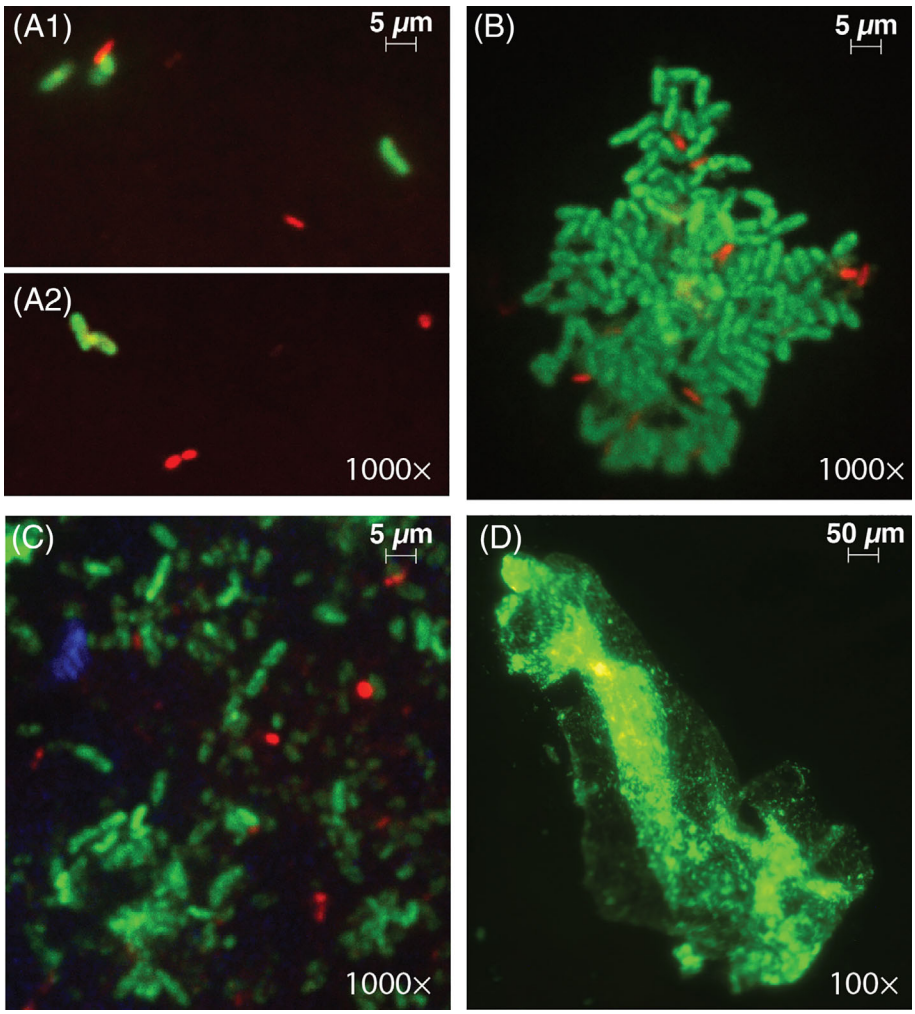

Fig 2. Representative images revealing stained cells (by CARD-FISH, see text for details) in the incubation experiments: (**A**) cells in pairs, (**B**) single-layer cluster, (**C**) multi-layer cluster, (**D**) sheet-like cluster. *Methylobacter* sp. is shown in green and *Methylotenera* sp. in red in panels A–C. The sample used for panel D was not stained for *Methylotenera* sp. cells and thus only *Methylobacter* sp. cells are visible (in green). Panels (**A1**) and (**A2**) show two separate images of the same incubation and microscope slide. The microscope magnification that was used is shown in the bottom-right corner of images.

a lake. It has been suggested that this partnership is affected by the amount of methanol generated from methane, released by the methanotroph, which was recently shown to be affected by lanthanides (Krause et al. 2017). Earlier studies have addressed the effect of oxygen on the co-occurrence of methanotrophs and non-methanotrophic methylotroph (Oshkin et al. 2014; Hernandez et al. 2015), but no other electron acceptors have been examined; nor were physical effects like aggregate formation evaluated. Here, we examined the effect of both chemical and physical factors on the methanotroph–methylotroph partnership, specifically on the suggested interaction between *Methylobacter–Methylotenera*.

The *Methylobacter* sp. that dominated the enrichment culture and the water column of Lacamas Lake, in both summer and winter, was shown to belong to the *Methylobacter* clade 2, with *Methylobacter tundripaludum* as the most closely related cultured relative (> 96% identical, van Grinsven et al. 2020*a*). The *Methylotenera* sp. present in the enrichment culture are closely related to species isolated from Lake Washington sediments (Kalyuzhnaya et al. 2006, 2011), as was determined by van Grinsven et al. (2020*b*). The co-occurrence of the two species was found in the water column of Lacamas Lake, in water column incubations, and in enrichment cultures obtained from the Lacamas Lake water column (R^2 = 0.7 for the linear regression of *Methylobacter* and *Methylotenera* spp. relative abundance), and also in sediment and Arctic lakes (He et al. 2012; Oshkin et al. 2014; de Jong et al. 2018; Fig. 4). This and the relative high abundance of these species suggests that this interaction may be relevant for the carbon transfer in lake food webs.

Carbon transfer from *Methylobacter* to *Methylotenera* cells

The presence of ^{13}C-labeled 16S rRNA gene sequences belonging to the non-methanotrophic *Methylotenera* sp. in

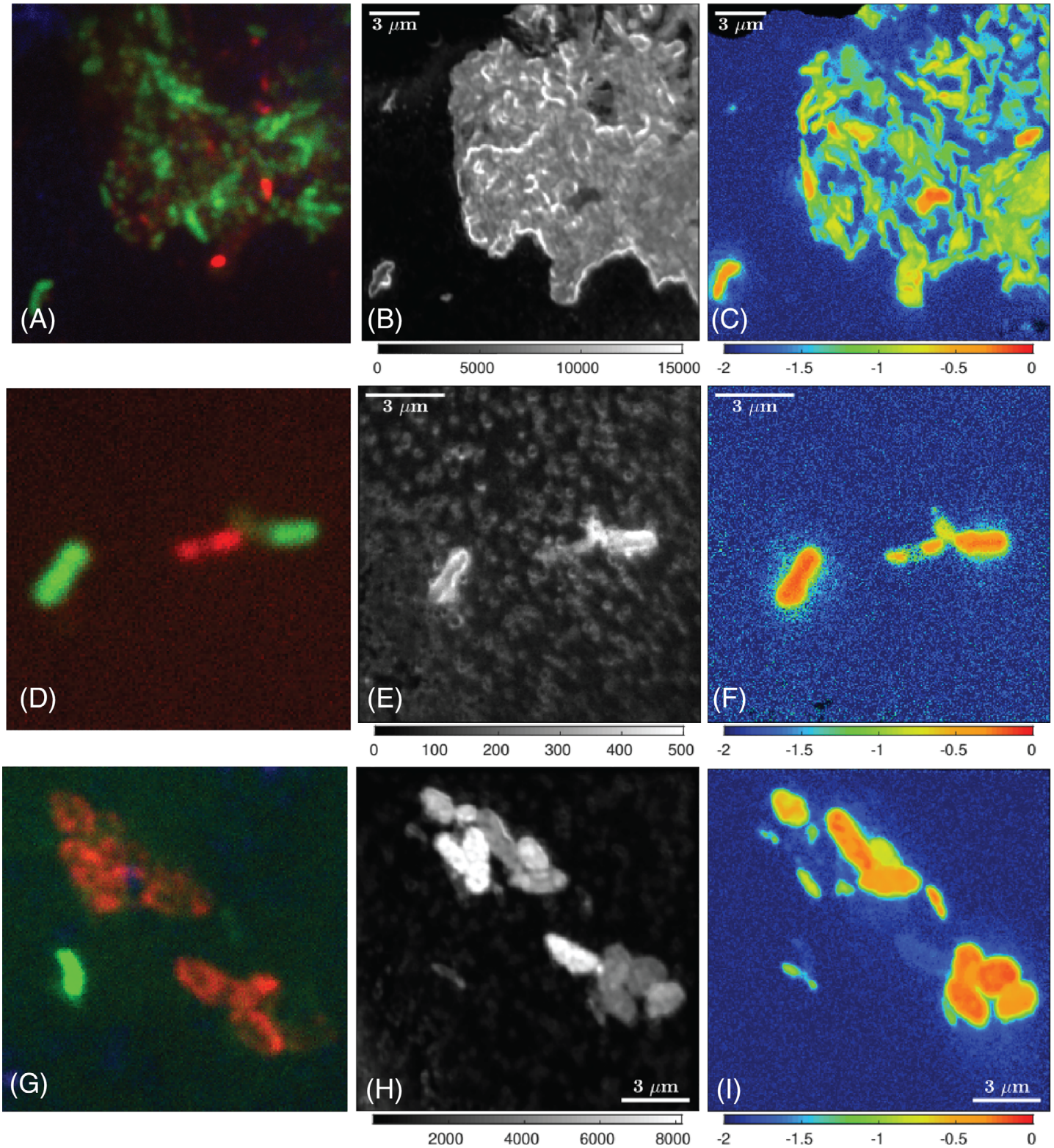

Fig 3. A large (**A–C**) and two small (**D–F**and**G–I**) cell clusters, consisting of*Methylobacter* sp. and *Methylotenera* sp. cells, detected in the incubation with nitrate. Panels (**A**), (**D**), and (**G**) show stained cells (by CARD-FISH, see text for details), with green cells representing *Methylobacter* sp. cells (Mlb482 probe) and red cells representing *Methylotenera* sp. cells (MET1216 probe). Panels (**B**), (**E**), and (**H**) show images of $^{12}C^{14}N$ ion counts, representing biomass distribution on the filter. Panels (**C**), (**F**), and (**I**) show the corresponding images of the ^{13}C atom fraction (calculated as $^{13}C^{14}N/(^{12}C^{14}N+^{13}C^{14}N)$, and shown in a log-scale for improved visibility), revealing the presence of methane-derived ^{13}C in both *Methylobacter* and *Methylotenera* cells. An overview of the $^{13}C^{14}N/(^{12}C^{14}N+^{13}C^{14}N)$ values of all measured cells is shown in Fig. S4.

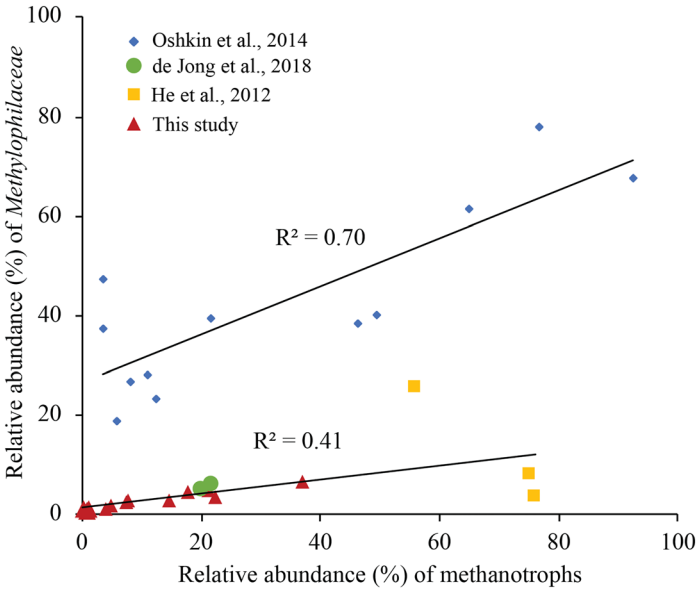

Fig 4. Methanotroph and *Methylophilacea* (which includes the genus *Methylotenera*) relative abundance in the water column and incubations of Lacamas lake, the source of the enrichment culture used in this study, as observed by van Grinsven et al. (2020*a*) (red triangles), in sediment incubation experiments by Oshkin et al. (2014) (blue diamonds), Arctic sediment enrichment cultures by de Jong et al. (2018) (green circles), and Arctic water column enrichment cultures by He et al. (2012) (yellow squares). The trendlines show the linear regression of the Oshkin et al. (2014) data (blue diamonds; upper trendline), and the combined linear regression of the de Jong et al. (2018), He et al. (2012) and van Grinsven et al. (2020a) data (lower trendline).

our oxic incubations supplemented with nitrate (Fig. 1) revealed the incorporation of methane-derived carbon into *Methylotenera* sp. Its genome does not encode the genes coding for particulate (pMMO) methane monooxygenase (*pmo*A gene; van Grinsven et al. 2020*b*) or the soluble methane monooxygenase (*sMMO*). This is consistent with the absence of both genes in any of the other published genomes of *Methylotenera* sp. (*M. mobilis* and *M. versatilis*; (Kalyuzhnaya et al. 2008, 2011; Lapidus et al. 2011). Therefore, a direct usage of the labeled methane by the *Methylotenera* sp. is highly unlikely. Labeled CO_2 or biomass, produced by methanotrophs, could potentially lead to indirect labeling (i.e., by scrambling) of community members, including *Methylotenera* sp. However, both autotrophic ^{13}C-CO_2 assimilation and heterotrophic consumption of ^{13}C-labeled biomass would only be expected to result in a low degree of labeling of the microbial community members. In contrast, we observed no enhanced labeling in non-methylotrophs (e.g., *Flavobacterium* sp.; Fig. 1), and a highly elevated labeling in the *Methylotenera* sp. We, therefore, expect *Methylotenera* sp. to use other highly labeled carbon substrates, that cannot be used by the majority of the community, rather than labeled CO_2. Break down of ^{13}C-labeled biomass and consumption of the degradation products, could have also resulted in labeling of non-methanotrophs, but the incubation experiments lasted only 2–3 d. Therefore, we expected labeled biomass degradation to be a minor component of labeled carbon cycling in our incubations.

The co-occurrence of *Methylobacter* and *Methylotenera* spp. in natural environments has been studied in sediments, soils and landfills, but not in the water column of lakes (Martineau et al. 2010; He et al. 2012; Beck et al. 2013). Based on previous studies (Kalyuhznaya et al. 2009; Krause et al. 2017), and on the genes of the carbon metabolism detected in the genome of the *Methylotenera* sp. present in our experiments (i.e., absence of the *pmoA* gene, presence of the genes encoding a complete methanol oxidation pathway; van Grinsven et al. 2020*b*), we suspect methanol to be the methane-derived component that is assimilated by *Methylotenera* sp. The production of methanol, by conversion of methane to methanol, is the first step in the methane oxidation process by methane oxidizing bacteria such as *Methylobacter* sp. (Fig. 5). Typically, methanol is further oxidized to formaldehyde, and the carbon is then assimilated or released as CO_2 (Fig. 5). Excretion of methanol by methanotrophs has been observed before, and was described as a mismatch between processes in the cell, producing more methanol than can be consumed, resulting in a release of methanol outside the cell (Tavormina et al. 2017). The release of methanol has been shown to lead to an energy deficiency in the methanotroph (Xin et al. 2004, 2007), resulting in a decreased methane oxidation rate. Previous studies have reported high free methanol concentrations in methanotroph cultures (up to 100 μM, Xin et al. 2004, 2007; Tavormina et al. 2017) that seem to inhibit further methanol production by the methanotrophic cells. If this is correct, the consumption of free methanol by *Methyloterena* sp. could stimulate activity of the methanotrophs, by removing the surplus of inhibitory methanol from the media. It remains unknown whether high methanol accumulation could also occur in the lake water column. Although some have suggested that carbon transfer from methanotrophs to methylotrophs is based on methanol exchange (Oshkin et al. 2014; Wei et al. 2016*a*), another study has also shown formaldehyde excretion and accumulation in the medium by methanotrophs under high oxygen concentrations (Costa et al. 2001), up to formaldehyde concentrations that inhibited the methanotrophs. As the oxygen concentration in our incubation experiments was high, it is possible that, as in Costa et al. (2001), formaldehyde was excreted by the *Methylobacter* sp. The removal of formaldehyde by the *Methylotenera* sp. could then enhance the methane oxidation rate by reducing the concentration of formaldehyde to subtoxic levels.

Spatial analysis of the *Methylobacter–Methylotenera* interaction

The NanoSIMS data of our study confirms our inferences based on our DNA-SIP data. Similar to the DNA-SIP data, the

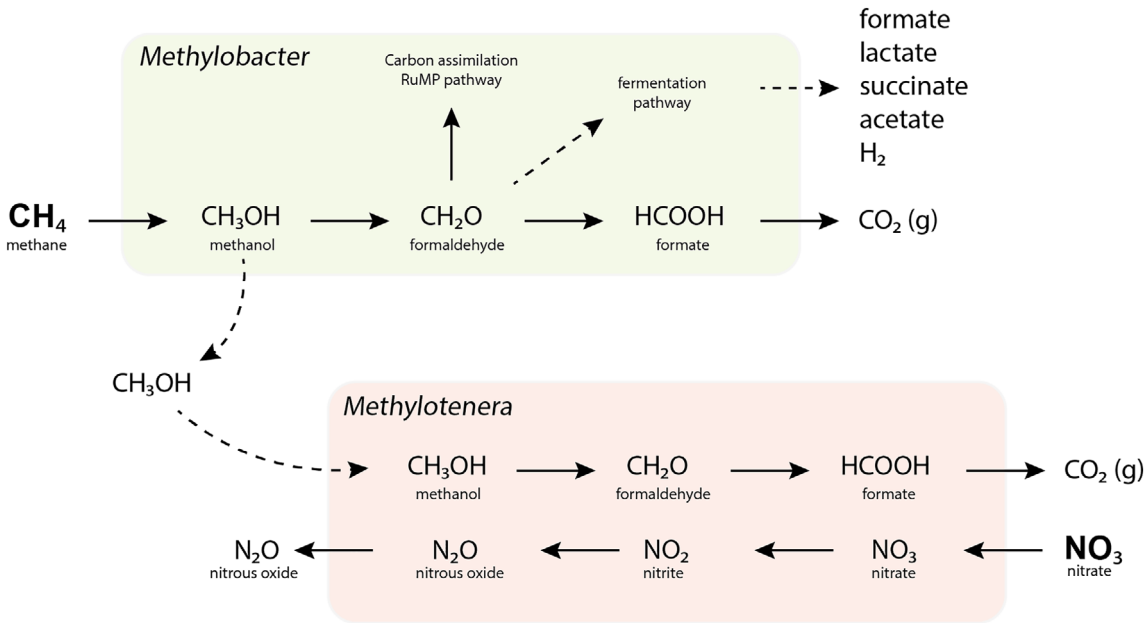

Fig 5. Schematic representation of the relevant pathways in the methanotroph *Methylobacter* sp. and in the methylotroph *Methylotenera* sp. Although energetically unfavorable for the methanotrophs, methane-derived carbon is expected to partially "leak" from the methanotroph after the conversion to methanol, to be used by the methylotroph *Methylotenera* sp. The methanol that does not leave the methanotroph cell is converted to formaldehyde, which is then partially used for carbon assimilation via the ribulose monophosphate (RuMP) pathway and partially leaves the cell as CO_2. Alternatively, in the case of oxygen limitation, formaldehyde can enter a fermentative pathway, eventually leaving the cell as mixed-acid fermentation products. Methanol is oxidized in *Methylotenera* sp., possibly coupled to the reduction of nitrate.

NanoSIMS data show that methane-derived carbon is assimilated by *Methylobacter* sp. as well as *Methylophilaceae* (according to 16S rRNA sequencing > 97% assigned to *Methylotenera* spp.) cells, and that no other community members got significantly ^{13}C-labeled (Fig. S4). In addition, the combination of CARD-FISH and NanoSIMS analyses was used to visualize the co-occurrence of *Methylobacter* and *Methylotenera* spp. for the first time. This data showed (^{13}C-labeled) *Methylobacter* and *Methylotenera* spp. in close vicinity (Fig. 2B, C; Fig. 3A–C), as well as physically separated (Figs. 2A, 3D–I), revealing that the suggested interaction between the methanotroph *Methylobacter* sp. and the methylotroph *Methylotenera* sp. is apparently independent of direct physical interaction of the two partners. We cannot exclude the possibility that the cell-distribution has changed due to the deposition and fixation process, but our data, which show a large number of single cells and clusters of only *Methylotenera* sp. cells (e.g., Fig. 2A,D), lead us to the believe that these distributions reflect the distributions in the enrichment culture.

The exchanged methane-derived carbon products could be dissolved in the medium, and reach the methylotrophs via diffusion. However, this would imply that these carbon-products are available free-for-all, which raises the question why specifically *Methylotenera* sp. can profit from these carbon-excretions, and no other methylotrophs. If the methane-derived carbon products are indeed released into the water column, and are thus freely accessible to other organisms, this could also have implications for the methane cycle from the production side, as these compounds could then be used for methylotrophic methanogenesis (Lovley and Klug 1983; Narrowe et al. 2019). Previously direct interspecies electron transfer has been shown to be important in the relationship between anaerobic methane oxidizing archaea and their syntrophic partners (Wegener et al. 2015; Krukenberg et al. 2018), and has additionally been suggested to occur between *Methylobacter* sp. and *Methylotenera* sp. (Yu and Chistoserdova 2017). However, the apparent lack of a cell-to-cell contact between part of the *Methylobacter* and *Methylotenera* cells, and the expectation that nanowires do not occur over these distances and in these species, make it unlikely that direct interspecies electron transfer played a role in the interaction between the free-living *Methylobacter* and *Methylotenera* cells in this study. However, for the cells in aggregates, as shown in Fig. 2B, direct interspecies electron transfer may occur.

Effect of nitrate on the *Methylobacter–Methylotenera* interaction

Collectively, the results of this study show, in line with the results of van Grinsven et al. (2020*b*), that nitrate stimulates methane oxidation by the methanotroph *Methylobacter*, and that products of methane oxidation by *Methylobacter* sp. are incorporated into the non-methanotrophic *Methylotenera* cells.

This carbon transfer between the methanotroph and non-methanotroph seems to occur under oxic conditions with nitrate, but not, or to a very limited degree, in the presence of ammonium. Similarly, in water column incubations enhanced methane oxidation rates were observed after the addition of nitrate (van Grinsven et al. 2020*a*,*b*), despite the much lower nitrate concentrations compared to our enrichment cultures. The nitrate concentration in the water column of eutrophic Lacamas Lake has been shown to vary strongly over the year (0.2–75 μM; Deemer et al. 2011; van Grinsven et al., 2020a), and the effect of nitrate on methane oxidation rates and carbon transfer may thus have important implications in the lake ecosystem. Ammonium can cause competitive inhibition of methane oxidation due to its structural similarity to methane (Bédard and Knowles 1989), although the much higher affinity of the methane monooxygenase enzyme for methane (600–1300-fold higher) likely limits this effect. Earlier studies have found both increases and decreases in the methane oxidation rate after ammonium addition (Bodelier et al. 2000; Walkiewicz et al. 2018), as well as for nitrate addition (Geng et al. 2017; Walkiewicz and Brzezińska 2019). The nitrate inhibitory effect observed in some other studies may be indirect, due to the conversion of nitrate to nitrite (Roco et al. 2016), which is known as an inhibitor of methane oxidation (Dunfield and Knowles 1995; Hütsch 1998). As high methane oxidation rates in both our ammonium and nitrate-amended incubations were observed, inhibition does not seem to be an important factor. It has been previously suggested that nitrate is used by methanotrophs for denitrification, based on the presence of the genes encoding for proteins involved in the denitrification pathway, which could be coupled to methane oxidation when oxygen is limiting (Smith et al. 2018). However, the genome of the *Methylobacter* sp. present in our incubations lacks the *nar* gene required to perform the dissimilatory conversion of nitrate to nitrite, as previously reported in van Grinsven et al. (2020*a*). We did detect, however, the *norBC* and *nirK* genes, encoding for part of the denitrification pathway, from nitrite to nitrous oxide, as well as the *nas* gene, encoding for nitrate to nitrite conversion in the assimilatory nitrate reduction pathway (van Grinsven et al. 2020*a*). Given the high seasonal nitrate inflow in eutrophic systems such as Lacamas Lake, the observed stimulation of *Methylobacter* sp. by the addition of nitrate could give these methanotrophs an advantage in occupying their niche. Possibly, the enhanced methane oxidation rates are related to the enhanced methane-derived carbon assimilation by *Methylotenera* sp. Only in the presence of nitrate, *Methylotenera* sp. seemed to assimilate significant amounts of methane-derived carbon. In the incubations with ammonium, DNA of *Methylotenera* sp. was not substantially labeled, despite its high relative abundance in those incubations (15.3%). In order to determine whether this could provide an explanation of the enhanced methane oxidation rates by nitrate addition, we explore what may cause the difference in behavior of *Methylotenera* sp. between the incubations with ammonium and nitrate. One explanation for the enhanced *Methylotenera* ^{13}C-labeling in the nitrate incubations could simply be enhanced activity of *Methylobacter* sp. in these incubations, causing a higher carbon substrate availability to *Methylotenera* sp. We, however, consider this unlikely as the major driver since the methane oxidation rate in the incubation experiments, and thus the production of methane-derived reaction products, was 2–4 times higher than in water column incubations, where we also observe a co-occurrence of *Methylobacter* sp. and *Methylotenera* sp. (van Grinsven et al. 2020*a*). The substrate availability to *Methylotenera* sp. is therefore expected to be sufficient in both the incubations with ammonium and nitrate. There could, however, be factors that affect the release of a reaction intermediate by *Methylobacter* cells, which is generally considered an unfavorable process for the *Methylobacter* sp. itself. Factors that are known to affect the methanol release by methanotrophic bacteria are the concentrations of lanthanides (Krause et al. 2017) and CO_2 (Xin et al. 2004) in the medium. We are, however, the first to suggest an effect of nitrate on the excretion of reaction intermediates. Another possibility is that the uptake of reaction products by *Methylotenera* sp. rather than the excretion (by *Methylobacter* sp.) is dependent on the presence of nitrate. Several studies have discussed whether nitrate is required for methanol oxidation by *Methylotenera* sp., and although an increase in relative abundance of *Methylotenera* sp. was observed in incubations with nitrate (Beck et al. 2013), none have shown an effect of nitrate on the incorporation of methane-derived ^{13}C-label. Mustakhimov et al. (2013) demonstrated the operation of an active denitrification pathway in *M. mobilis* under oxic conditions, although denitrification was not essential for its methanol metabolism.

Genome analysis of the *Methylotenera* sp. present in our incubations revealed the presence of the genes encoding for nitrate transporters, assimilatory nitrate reductase (Nas) to nitrite, nitrite reductase (NirBD) to ammonia, and to nitric oxide (NirK), as well as the gene coding for the nitric oxide reductase (NorBC) to nitrous oxide (N_2O) (van Grinsven et al. 2020*b*). No dissimilatory nitrate reductase genes were annotated, but we explored the potential role of the detected assimilatory Nas gene in dissimilatory nitrate reduction. The Nas gene of our *Methylotener*a sp. genome is 90% identical (905 amino acid positions) to the molybdopterin oxidoreductase of *M. mobilis* JLW8 (Mmol_1648) (Mustakhimov et al. 2013). This Nap is likely involved in both the assimilatory and the dissimilatory denitrification pathways, based on experiment with mutants lacking this gene. Both the nitrate reductase detected in our *Methylotenera* sp. genome as well as that of *M. mobilis* JLW8 have a region "MopB_CT_Nitrate-R-NapA-like" that supports its relationship with periplasmatic NapA nitrate reductases. However, a prediction by the CELLO V.2.5 subcellular location prediction tool of the cellular locations of the nitrate reductases of both *M. mobilis* JLW8

(Mmol_1648) and our *Methylotenera* sp. suggested these nitrate reductases have a cytoplasmatic location (2.9 score for cytoplasmatic location vs. a 1.3 score for periplasmatic location, for both *Methylotenera* spp.) and are therefore not expected to be membrane or periplasmatic-located dissimilatory nitrate reductases. More studies are required to determine the physiological role of these nitrate reductases.

In addition to their ecosystem and carbon-cycling implications, our results also have potential relevance to wastewater treatment, where aerobic methane oxidation-coupled denitrification could be used for efficient removal of both methane and nitrate from waste (Modin et al. 2008; Zhu et al. 2016). More research is needed to determine whether the *Methylobacter–Methylotenera* interaction that is suggested by this study, would be suitable for such an industrial application.

Conclusions

Here, we show that cross-feeding on methane-derived carbon seems to be an important driver for the relationship between *Methylobacter* sp. and *Methylotenera* sp., and a possible gain for *Methylobacter* sp. would be the removal of toxic compounds that inhibit methanotrophy. As no physical contact seems to be required for the *Methylobacter–Methylotenera* interaction, an exchange of electrons between the two species seems unlikely, as well as any other direct exchange of compounds. Released compounds are more likely to be freely available in the medium. Earlier research has shown that *Methylotenera* sp. can actively affect the methanol dehydrogenase gene expression in *Methylobacter* sp. (Krause et al. 2017), and our research suggests that nitrate is an important factor in this interaction. More research on the pathways, mechanisms and potential beneficial effects for *Methylobacter* sp. is, however, required.

The observed nitrate-dependence of methane-derived carbon incorporation into *Methylotenera* sp. is novel and may be relevant for culture and ecosystems studies, especially given the stimulating effect of nitrate on methane oxidation rates that was observed before in the Lacamas Lake water column. The *Methylobacter–Methylotenera* interaction could play a role in linking the carbon and nitrogen cycles of methane-rich lakes, with implications for the transfer of methane-derived carbon through the trophic levels of lake food webs.

References

Andrews, S., F. Krueger, A. Seconds-Pichon, F. Biggins, and S. Wingett (2015) FastQC. A quality control tool for high throughput sequence data. Babraham bioinformatics. Babraham Inst 1: 1.

Asbun, A. A., M. A. Besseling, S. Balzano, J. van Bleijswijk, H. Witte, L. Villanueva, and J. C. Engelmann. 2019. Cascabel: A flexible, scalable and easy-to-use amplicon sequence data analysis pipeline. BioRxiv **809384**. doi:10.1101/809384

Bastviken, D., J. J. Cole, M. L. Pace, and M. C. van de Bogert. 2008. Fates of methane from different lake habitats: Connecting whole-lake budgets and CH4 emissions. J. Geophys. Res. Biogeo. **113**: 1–13. doi:10.1029/2007JG000608

Bastviken, D., L. J. Tranvik, J. A. Downing, P. M. Crill, and A. Enrich-Prast. 2011. Freshwater methane emissions offset the continental carbon sink. Science **331**: 50. doi:10.1126/science.1196808

Beck, D. A. C., E. L. Hendrickson, A. Vorobev, T. Wang, S. Lim, M. G. Kalyuzhnaya, M. E. Lidstrom, M. Hackett, and L. Chistoserdova. 2011. An integrated proteomics/transcriptomics approach points to oxygen as the main electron sink for methanol metabolism in *Methylotenera mobilis*. J. Bacteriol. **193**: 4758–4765. doi:10.1128/JB.05375-11

Beck, D. A. C., M. G. Kalyuzhnaya, S. Malfatti, S. G. Tringe, T. Glavina del Rio, N. Ivanova, M. E. Lidstrom, and L. Chistoserdova. 2013. A metagenomic insight into freshwater methane-utilizing communities and evidence for cooperation between the Methylococcaceae and the Methylophilaceae. PeerJ **1**: e23. doi:10.7717/peerj.23

Bédard, C., and R. Knowles. 1989. Physiology, biochemistry, and specific inhibitors of CH4, NH4+, and CO oxidation by methanotrophs and nitrifiers. Microbiol. Rev. **53**: 68–84.

Bodelier, P. L. E., P. Roslev, T. Henckel, and P. Frenzel. 2000. Stimulation by ammonium-based fertilizers of methane oxidation in soil around rice roots. Nature **403**: 421–424. doi:10.1038/35000193

Bowman, J. P., L. I. Sly, P. D. Nichols, and A. C. Hayward. 1994. Revised taxonomy of the methanotrophs: Description of Methylobacter gen. nov., emendation of Methylococcus, validation of Methylosinus and Methylocystis species, and a proposal that the family Methylococcaceae includes only the group I methanotrophs. Int. J. Syst. Bacteriol. **44**: 375–375. doi:10.1099/00207713-44-2-375

Caporaso, J. G., and others. 2012. Ultra-high-throughput microbial community analysis on the Illumina HiSeq and MiSeq platforms. ISME J. **6**: 1621–1624. doi:10.1038/ismej.2012.8

Costa, C., M. Vecherskaya, C. Dijkema, and A. J. M. Stams. 2001. The effect of oxygen on methanol oxidation by an obligate methanotrophic bacterium studied by in vivo 13C nuclear magnetic resonance spectroscopy. J. Ind. Microbiol. Biotechnol. **26**: 9–14. doi:10.1038/sj.jim.7000075

de Jong, A. E. E., M. H. In 't Zandt, O. H. Meisel, M. S. M. Jetten, J. F. Dean, O. Rasigraf, and C. U. Welte. 2018. Increases in temperature and nutrient availability positively affect methane-cycling microorganisms in Arctic thermokarst lake sediments. Environ. Microbiol. **20**: 4314–4327. doi:10.1111/1462-2920.14345

Deemer, B. R., J. a. Harrison, and E. W. Whitling. 2011. Microbial dinitrogen and nitrous oxide production in a small eutrophic reservoir: An in situ approach to quantifying hypolimnetic process rates. Limnol. Oceanogr. **56**: 1189–1199. doi:10.4319/lo.2011.56.4.1189

Deemer, B. R., and others. 2016. Greenhouse gas emissions from reservoir water surfaces: A new global synthesis. Bioscience **66**: 949–964. doi:10.1093/biosci/biw117

DelSontro, T., J. J. Beaulieu, and J. A. Downing. 2018. Greenhouse gas emissions from lakes and impoundments: Upscaling in the face of global change. Limnol. Oceanogr. Lett. **3**: 64–75. doi:10.1002/lol2.10073

Dunfield, P., and R. Knowles. 1995. Kinetics of inhibition of methane oxidation by nitrate, nitrite, and ammonium in a humisol. Appl. Environ. Microbiol. **61**: 3129–3135.

Dunford, E. A., and J. D. Neufeld. 2010. DNA stable-isotope probing (DNA-SIP). J. Vis. Exp. **42**: e2027. doi:10.3791/2027

Ettwig, K. F., M. K. Butler, D. Le Paslier, E. Pelletier, S. Mangenot, M. M. M. Kuypers, et al. 2010. Nitrite-driven anaerobic methane oxidation by oxygenic bacteria. Nature **464**: 543–548. doi:10.1038/nature08883

Geng, J., S. Cheng, H. Fang, G. Yu, X. Li, G. Si, S. He, and G. Yu. 2017. Soil nitrate accumulation explains the nonlinear responses of soil CO_2 and CH_4 fluxes to nitrogen addition in a temperate needle-broadleaved mixed forest. Ecol. Indic. **79**: 28–36. doi:10.1016/j.ecolind.2017.03.054

He, R., M. J. Wooller, J. W. Pohlman, J. Quensen, J. M. Tiedje, and M. B. Leigh. 2012. Diversity of active aerobic methanotrophs along depth profiles of arctic and subarctic lake water column and sediments. ISME J. **6**: 1937–1948. doi:10.1038/ismej.2012.34

He, R., M. J. Wooller, J. W. Pohlman, J. M. Tiedje, and M. B. Leigh. 2015. Methane-derived carbon flow through microbial communities in arctic lake sediments. Environ. Microbiol. **17**: 3233–3250. doi:10.1111/1462-2920.12773

Hernandez, M. E., D. A. C. Beck, M. E. Lidstrom, and L. Chistoserdova. 2015. Oxygen availability is a major factor in determining the composition of microbial communities involved in methane oxidation. PeerJ **3**: e801. doi:10.7717/peerj.801

Hütsch, B. W. 1998. Methane oxidation in arable soil as inhibited by ammonium, nitrite, and organic manure with respect to soil pH. Biol. Fertil. Soils **28**: 27–35. doi:10.1007/s003740050459

Jones, R. I., and J. Grey. 2011. Biogenic methane in freshwater food webs. Freshw. Biol. **56**: 213–229. doi:10.1111/j.1365-2427.2010.02494.x

Jones, R. I., J. Grey, D. Sleep, and L. Arvola. 1999. Stable isotope analysis of zooplankton carbon nutrition in Humic Lakes. Oikos **86**: 97–104. doi:10.2307/3546573

Kalyuzhnaya, M. G., S. Bowerman, J. C. Lara, M. E. Lidstrom, and L. Chistoserdova. 2006. *Methylotenera mobilis* gen. nov., sp. nov., an obligately methelamine-utilizing bacterium within the family Methylophilaceae. Int. J. Syst. Evol. Microbiol. **56**: 2819–2823. doi:10.1099/ijs.0.64191-0

Kalyuzhnaya, M. G., and others. 2008. High-resolution metagenomics targets specific functional types in complex microbial communities. Nat. Biotechnol. **26**: 1029–1034. doi:10.1038/nbt.1488

Kalyuhznaya, M. G., W. Martens-Habbena, T. Wang, M. Hackett, S. M. Stolyar, D. A. Stahl, M. E. Lidstrom, and L. Chistoserdova. 2009. Methylophilaceae link methanol oxidation to denitrification in freshwater lake sediment as suggested by stable isotope probing and pure culture analysis. Environ. Microbiol. Rep. **1**: 385–392. doi:10.1111/j.1758-2229.2009.00046.x

Kalyuzhnaya, M. G., D. A. C. Beck, A. Vorobev, N. Smalley, D. D. Kunkel, M. E. Lidstrom, and L. Chistoserdova. 2011. Novel methylotrophic isolates from lake sediment, description of Methylotenera versatilis sp. nov. and emended description of the genus Methylotenera. Int. J. Syst. Evol. Microbiol. **62**: 106–111. doi:10.1099/ijs.0.029165-0

Kalyuzhnaya, M. G., S. Yang, O. N. Rozova, N. E. Smalley, J. Clubb, A. Lamb, and others. 2013. Highly efficient methane biocatalysis revealed in a methanotrophic bacterium. Nat. Commun. **4**: 1–7. doi:10.1038/ncomms3785

van Grinsven, S., J. S. Sinninghe Damsté, A. Abdala Asbun, J. C. Engelmann, J. Harrison, and L. Villanueva. 2020*a*. Methane oxidation in anoxic lake water stimulated by nitrate and sulfate addition. Environ. Microbiol. **22**: 766–782. doi:10.1111/1462-2920.14886

van Grinsven, S., J. S. Sinninghe Damsté, J. Harrison, and L. Villanueva. 2020*b*. Impact of electron acceptor availability on methane-influenced microorganisms in an enrichment culture obtained from a stratified lake. Front Microbiol: 11. doi:10.3389/fmicb.2020.00715

Khmelenina, V. N., V. N. Shchukin, A. S. Reshetnikov, I. I. Mustakhimov, N. E. Suzina, B. T. Eshinimaev, and Y. A. Trotsenko. 2010. Structural and functional features of methanotrophs from hypersaline and alkaline lakes. Microbiology **79**: 472–482. doi:10.1134/S0026261710040090

Kits, K. D., M. G. Klotz, and L. Y. Stein. 2015. Methane oxidation coupled to nitrate reduction under hypoxia by the Gammaproteobacterium Methylomonas denitrificans, sp. nov. type strain FJG1. Environ. Microbiol. **17**: 3219–3232. doi:10.1111/1462-2920.12772

Krause, S. M. B., T. Johnson, Y. S. Karunaratne, Y. Fu, D. A. C. Beck, L. Chistoserdova, and M. E. Lidstrom. 2017. Lanthanide-dependent cross-feeding of methane-derived carbon is linked by microbial community interactions. Proc. Natl. Acad. Sci. U. S. A. **114**: 358–363. doi:10.1073/pnas.1619871114

Krukenberg, V., D. Riedel, H. R. Gruber-Vodicka, P. L. Buttigieg, H. E. Tegetmeyer, A. Boetius, and G. Wegener. 2018. Gene expression and ultrastructure of meso- and thermophilic methanotrophic consortia. Environ. Microbiol. **20**: 1651–1666. doi:10.1111/1462-2920.14077

Lapidus, A., and others. 2011. Genomes of three methylotrophs from a single niche reveal the genetic and metabolic divergence of the methylophilaceae. J. Bacteriol. **193**: 3757–3764. doi:10.1128/JB.00404-11

Lovley, D. R., and M. J. Klug. 1983. Methanogenesis from methanol and methylamines and acetogenesis from hydrogen and carbon dioxide in the sediments of a eutrophic lake. Appl. Environ. Microbiol. **45**: 1310–1315.

Martineau, C., L. G. Whyte, and C. W. Greer. 2010. Stable isotope probing analysis of the diversity and activity of methanotrophic bacteria in soils from the Canadian high Arctic. Appl. Environ. Microbiol. **76**: 5773–5784. doi:10.1128/AEM.03094-09

Modin, O., K. Fukushi, F. Nakajima, and K. Yamamoto. 2008. A membrane biofilm reactor achieves aerobic methane oxidation coupled to denitrification (AME-D) with high efficiency. Water Sci. Technol. **58**: 83–87. doi:10.2166/wst.2008.648

Murase, J., and P. Frenzel. 2007. A methane-driven microbial food web in a wetland rice soil. Environ. Microbiol. **9**: 3025–3034. doi:10.1111/j.1462-2920.2007.01414.x

Murrell, J. C. 2010. The aerobic methane oxidizing bacteria (Methanotrophs), p. 1953–1966. *In* Handbook of hydrocarbon and lipid microbiology. Springer Berlin Heidelberg

Mustakhimov, I., M. G. Kalyuzhnaya, M. E. Lidstrom, and L. Chistoserdova. 2013. Insights into denitrification in *Methylotenera mobilis* from denitrification pathway and methanol metabolism mutants. J. Bacteriol. **195**: 2207–2211. doi:10.1128/JB.00069-13

Narrowe, A. B., M. A. Borton, D. W. Hoyt, G. J. Smith, R. A. Daly, J. C. Angle, et al. 2019. Uncovering the diversity and activity of Methylotrophic methanogens in freshwater wetland soils. mSystems **4**: 1–15. doi:10.1128/mSystems.00320-19

Oshkin, I. Y., D. A. Beck, A. E. Lamb, V. Tchesnokova, G. Benuska, T. L. McTaggart, and others. 2014. Methane-fed microbial microcosms show differential community dynamics and pinpoint taxa involved in communal response. ISME J. **9**: 1–11. doi:10.1038/ismej.2014.203

Polerecky, L., B. Adam, J. Milucka, N. Musat, T. Vagner, and M. M. M. Kuypers. 2012. Look@NanoSIMS - A tool for the analysis of nanoSIMS data in environmental microbiology. Environ. Microbiol. **14**: 1009–1023. doi:10.1111/j.1462-2920.2011.02681.x

Quast, C., E. Pruesse, P. Yilmaz, J. Gerken, T. Schweer, P. Yarza, J. Peplies, and F. O. Glöckner. 2013. The SILVA ribosomal RNA gene database project: Improved data processing and web-based tools. Nucleic Acids Res. **41**: D590–D596. doi:10.1093/nar/gks1219

Roco, C. A., L. L. Bergaust, J. P. Shapleigh, and J. B. Yavitt. 2016. Reduction of nitrate to nitrite by microbes under oxic conditions. Soil Biol. Biochem. **100**: 1–8. doi:10.1016/j.soilbio.2016.05.008

Sanseverino, A. M., D. Bastviken, I. Sundh, J. Pickova, and A. Enrich-Prast. 2012. Methane carbon supports aquatic food webs to the fish level. PLoS One **7**: e42723. doi:10.1371/journal.pone.0042723

Saunois, M., and others. 2016. The global methane budget 2000–2012. Earth Syst. Sci. Data **8**: 697–751. doi:10.5194/essd-8-697-2016

Saxton, M. A., V. A. Samarkin, C. A. Schutte, M. W. Bowles, M. T. Madigan, S. B. Cadieux, L. M. Pratt, and S. B. Joye. 2016. Biogeochemical and 16S rRNA gene sequence evidence supports a novel mode of anaerobic methanotrophy in permanently ice-covered Lake Fryxell, Antarctica. Limnol. Oceanogr. **61**: S119–S130. doi:10.1002/lno.10320

Schubert, C. J., F. Vazquez, T. Loesekann-Behrens, K. Knittel, M. Tonolla, and A. Boetius. 2011. Evidence for anaerobic oxidation of methane in sediments of a freshwater system (Lago di Cadagno). FEMS Microbiol. Ecol. **76**: 26–38. doi:10.1111/j.1574-6941.2010.01036.x

Smith, G. J., J. C. Angle, L. M. Solden, R. A. Daly, M. D. Johnston, M. A. Borton, and others. 2018. Members of the genus Methylobacter are inferred to account for the majority of aerobic methane oxidation in oxic soils from a freshwater wetland. MBio **9**: 1–17. doi:10.1128/mbio.00815-18

Smith, K. S., A. M. Costello, and M. E. Lidstrom. 1997. Methane and trichloroethylene oxidation by an estuarine methanotroph, Methylobacter sp. strain BB5.1. Appl. Environ. Microbiol. **63**: 4617–4620.

Stocker, T. F., and others. 2013. IPCC, 2013: Summary for policymakers. *In* Climate Change 2013: The physical science basis. Contribution of working group I to the fifth assessment report of the Intergovernmental panel on climate change. Cambridge, United Kingdom: *Cambridge Univ Press*.

Suominen, S., N. Dombrowski, J. S. Sinninghe Damsté, and L. Villanueva. 2020. A diverse uncultivated microbial community is responsible for organic matter degradation in the Black Sea sulphidic zone. Environ. Microbiol. doi:10.1111/1462-2920.14902

Taipale, S., P. Kankaala, M. Hahn, R. Jones, and M. Tiirola. 2011. Methane-oxidizing and photoautotrophic bacteria are major producers in a humic lake with a large anoxic hypolimnion. Aquat. Microb. Ecol. **64**: 81–95. doi:10.3354/ame01512

Tavormina, P. L., and others. 2017. Starvation and recovery in the deep-sea methanotroph *Methyloprofundus sedimenti*. Mol. Microbiol. **103**: 242–252. doi:10.1111/mmi.13553

Walkiewicz, A., M. Brzezińska, and A. Bieganowski. 2018. Methanotrophs are favored under hypoxia in ammonium-fertilized soils. Biol. Fertil. Soils **54**: 861–870. doi:10.1007/s00374-018-1302-9

Walkiewicz, A., and M. Brzezińska. 2019. Interactive effects of nitrate and oxygen on methane oxidation in three different soils. Soil Biol. Biochem. **133**: 116–118. doi:10.1016/j.soilbio.2019.03.001

Wartiainen, I., A. G. Hestnes, I. R. McDonald, and M. M. Svenning. 2006. Methylobacter tundripaludum sp. nov., a methane-oxidizing bacterium from Arctic wetland soil on the Svalbard islands, Norway (78° N). Int. J. Syst. Evol. Microbiol. **56**: 109–113. doi:10.1099/ijs.0.63728-0

Wegener, G., V. Krukenberg, D. Riedel, H. E. Tegetmeyer, and A. Boetius. 2015. Intercellular wiring enables electron transfer between methanotrophic archaea and bacteria. Nature **526**: 587–590. doi:10.1038/nature15733

Wei, X. M., R. He, M. Chen, Y. Su, and R. C. Ma. 2016*a*. Conversion of methane-derived carbon and microbial community in enrichment cultures in response to O2-availability. Environ. Sci. Pollut. Res. **23**: 7517–7528. doi:10.1016/j.apsoil.2016.01.009

Wei, M., Q. Qiu, Y. Qian, L. Cheng, and A. Guo. 2016*b*. Methane oxidation and response of Methylobacter/Methylosarcina methanotrophs in flooded rice soil amended with urea. Appl. Soil Ecol. **101**: 174–184. doi:10.1007/s11356-015-6017-y

Whittenbury, R., K. C. Phillips, and J. F. Wilkinson. 1970. Enrichment, isolation and some properties of methane-utilizing bacteria. J. Gen. Microbiol. **61**: 205–218. doi:10.1099/00221287-61-2-205

Xin, J. Y., J. R. Cui, J. Z. Niu, S. F. Hua, C. G. Xia, S. B. Li, and L. M. Zhu. 2004. Production of methanol from methane by methanotrophic bacteria. Biocatal. Biotransformation **22**: 225–229. doi:10.1080/10242420412331283305

Xin, J. Y., Y. X. Zhang, S. Zhang, C. G. Xia, and S. B. Li. 2007. Methanol production from CO_2 by resting cells of the methanotrophic bacterium *Methylosinus trichosporium* IMV 3011. J. Basic Microbiol. **47**: 426–435. doi:10.1002/jobm.200710313

Yu, Z., and L. Chistoserdova. 2017. Communal metabolism of methane and the rare earth element switch. J. Bacteriol. **199**: e00328–e00317. doi:10.1128/jb.00328-17

Yvon-Durocher, G., A. P. Allen, D. Bastviken, R. Conrad, C. Gudasz, A. St-Pierre, N. Thanh-Duc, and P. A. del Giorgio. 2014. Methane fluxes show consistent temperature dependence across microbial to ecosystem scales. Nature **507**: 488–491. doi:10.1038/nature13164

Zhang, J., K. Kobert, T. Flouri, and A. Stamatakis. 2014. PEAR: A fast and accurate illumina paired-end reAd mergeR. Bioinformatics **30**: 614–620. doi:10.1093/bioinformatics/btt593

Zhu, J., Q. Wang, M. Yuan, G. A. Tan, F. Sun, C. Wang, and others. 2016. Microbiology and potential applications of aerobic methane oxidation coupled to denitrification (AME-D) process: A review. Water Res. **90**: 203–215. doi:10.1016/j.watres.2015.12.020

Acknowledgments

We thank Keith Birchfield for sample collection, Michiel Kienhuis (Utrecht University NanoSIMS facility) for NanoSIMS analysis, Ilya Grigoriev (Utrecht University Biology Imaging Centre) for help with fluorescence microscopy and photo-ablation, Alejandro Abdala Asbun for help with bioinformatic analyses, and Saara Suominen, Sanne Vreugdenhil and Maartje Brouwer for help with DNA-SIP analyses. We also thank Cornelia Welte and two anonymous referees for helpful comments on earlier drafts of this manuscript. This work was supported by the Soehngen Institute of Anaerobic Microbiology (SIAM) Gravitation grant (024.002.002) of the Netherlands Ministry of Education, Culture and Science (OCW) and the Netherlands Organization for Scientific Research (NWO) to JSSD and LV. The NanoSIMS facility at Utrecht University was financed through a large infrastructure grant (175.010.2009.011) by NWO.

Conflict of Interest

None declared.

Submitted 14 February 2020
Revised 14 July 2020
Accepted 19 October 2020

Associate editor: Ronnie N. Glud